



OPEN ACCESS

EDITED BY

Michael Lupberger, University of Bonn, Germany

Maurizio Bonesini.

National Institute of Nuclear Physics of Milano

Bicocca, Italy

Jacopo Pazzini,

University of Padua, Italy

Giovanni Carugno,

National Institute of Nuclear Physics of Padova, Italy

*CORRESPONDENCE

Adam John Lowe,

alowe@liverpool.ac.uk

RECEIVED 13 March 2025

ACCEPTED 30 September 2025 PUBLISHED 20 October 2025

Martinez PA, Deisting A, Gatti HF, González-Díaz D, Lowe AJ, Majumdar K, Mavrokoridis K. Nessi M. Philippou B. Pietropaolo F, Ravinthiran S, Resnati F, Roberts A, Hernández AS, Touramanis C and Vann J (2025) Design and performance of the ARIADNE⁺ detector, bringing novel 3D optical dual-phase LArTPCs to the large scale. Front, Detect. Sci. Technol. 3:1593087. doi: 10.3389/fdest.2025.1593087

COPYRIGHT

© 2025 Martinez, Deisting, Gatti, González-Díaz, Lowe, Majumdar, Mayrokoridis, Nessi, Philippou, Pietropaolo, Ravinthiran, Resnati, Roberts, Hernández, Touramanis and Vann. This is an open-access article distributed under the terms of the Creative Commons Attribution License (CC BY). The use, distribution or reproduction in other forums is permitted. provided the original author(s) and the copyright owner(s) are credited and that the original publication in this journal is cited, in accordance with accepted academic practice. No use, distribution or reproduction is permitted which does not comply with these

Design and performance of the ARIADNE+ detector, bringing novel 3D optical dual-phase LArTPCs to the large scale

Pablo Amedo Martinez¹, Alexander Deisting², Heriques Frandini Gatti³, Diego González-Díaz¹, Adam John Lowe^{3*}, Krishanu Majumdar³, Konstantinos Mavrokoridis³, Marzio Nessi⁴, Barney Philippou³, Francesco Pietropaolo⁴, Sudikshan Ravinthiran³, Filippo Resnati⁴, Adam Roberts³, Angela Saá Hernández¹, Christos Touramanis³ and Jared Vann³

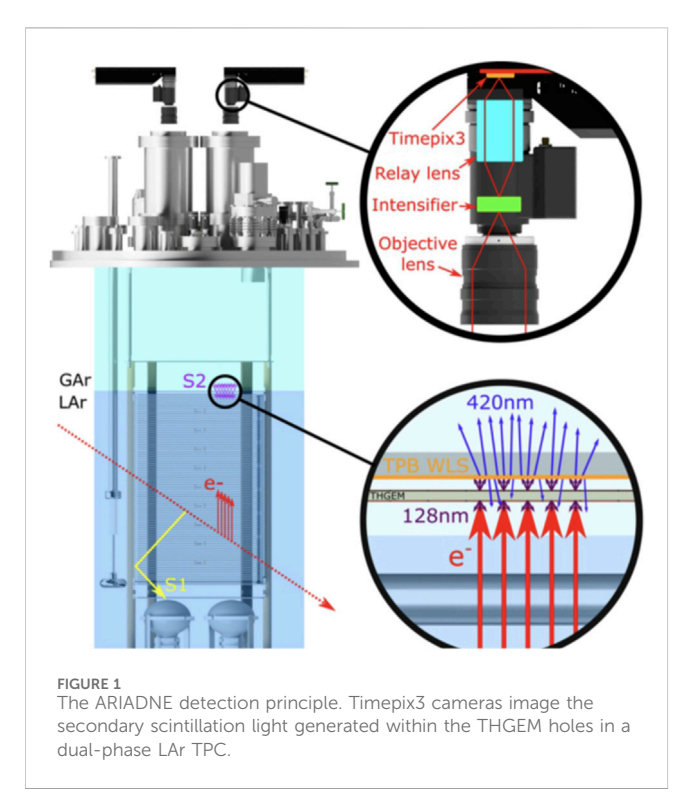
¹Instituto Galego de Física de Altas Enerxías, Universidade de Santiago de Compostela, Santiago de Compostela, Spain, ²Institute of Physics, Johannes Gutenberg University Mainz, Mainz, Germany, ³Department of Physics, University of Liverpool, Liverpool, United Kingdom, ⁴European Organization for Particle Physics (CERN), Geneva, Switzerland

The ARIADNE programme is focused on the development of a scalable optical readout system for use in future ktonne LAr neutrino experiments, providing high tracking capability and low energy thresholds. Following demonstration at the 1 tonne scale (ARIADNE detector), a 20 tonne experiment has been performed at the CERN Neutrino Platform (ARIADNE⁺) to test scalability for integration into colossal future experiments such as those planned within the DUNE programme. This paper details the design, construction and performance of a 2.3×2.3 m light readout plane (LRP), which contained the largest glass THGEM array ever constructed. Four Timepix3 cameras were mounted externally to image the secondary scintillation light produced within the THGEM holes; three cameras operated with a visible image intensifier, and one with a VUV sensitive intensifier coupled to a custom magnesium fluoride lens. The Timepix3 data are natively zero suppressed, and with the 1.6 ns timing resolution, straightforward 3D event reconstruction is possible. A gallery of reconstructed LAr interactions is presented. Energy resolution and calibration were determined using cosmic muons. The energy resolution was found to be approximately 11% for the presented dataset. An outlook on the next steps for this work is given.

time projection chambers (TPC), noble liquid detectors, micropattern gaseous detectors, glass thick gaseous electron multipliers (G-THGEMs), photon detectors for UV, visible and IR photons (solid-state)

1 Introduction

Traditional wire-based readout methods for Liquid Argon Time Projection Chambers (LAr TPCs) are facing a number of engineering and technological challenges as the nextgeneration of LAr neutrino experiments see ktonne-scale active volumes. These challenges stem from the various experimental requirements such as spatial resolution and energy



thresholds. Therefore, alternative methods of readout are now being looked at to both compliment existing technologies and offer cost-efficient solutions without sacrificing performance. A detailed comparison of LAr TPC readout methods, including the optical readout approach described in this paper, is available in (Majumdar and Mavrokoridis, 2021).

The ARIADNE program has successfully demonstrated the viability of optical readout for dual-phase LAr TPCs using fast, high resolution Timepix3 cameras (Fisher-Levine and Nomerotski, 2016). This includes the readout of the 1 tonne ARIADNE detector at Liverpool with the use of a Thick Gaseous Electron Multiplier (THGEM) to image through-going muons (Hollywood et al., 2020; Lowe et al., 2020). Demonstrating the further scalability of ARIADNE technology is vital if this technology is to be considered an option for large-scale neutrino experiments such as DUNE (DUNE Collaboration, 2018).

Built for testing the vertical drift Charge Readout Planes (CRPs) (DUNE Collaboration, 2023), the ProtoDUNE "cold box" offers an ideal test bed for a modular ARIADNE Light Readout Plane (LRP). This paper begins with an overview of the ARIADNE detection principle and how this approach was scaled up for ARIADNE⁺. The novel components which make up the LRP are detailed along with the assembly of the detector. Finally, the operation of the detector, data acquisition and calibration results are given.

2 Materials and methods

2.1 ARIADNE detection principle

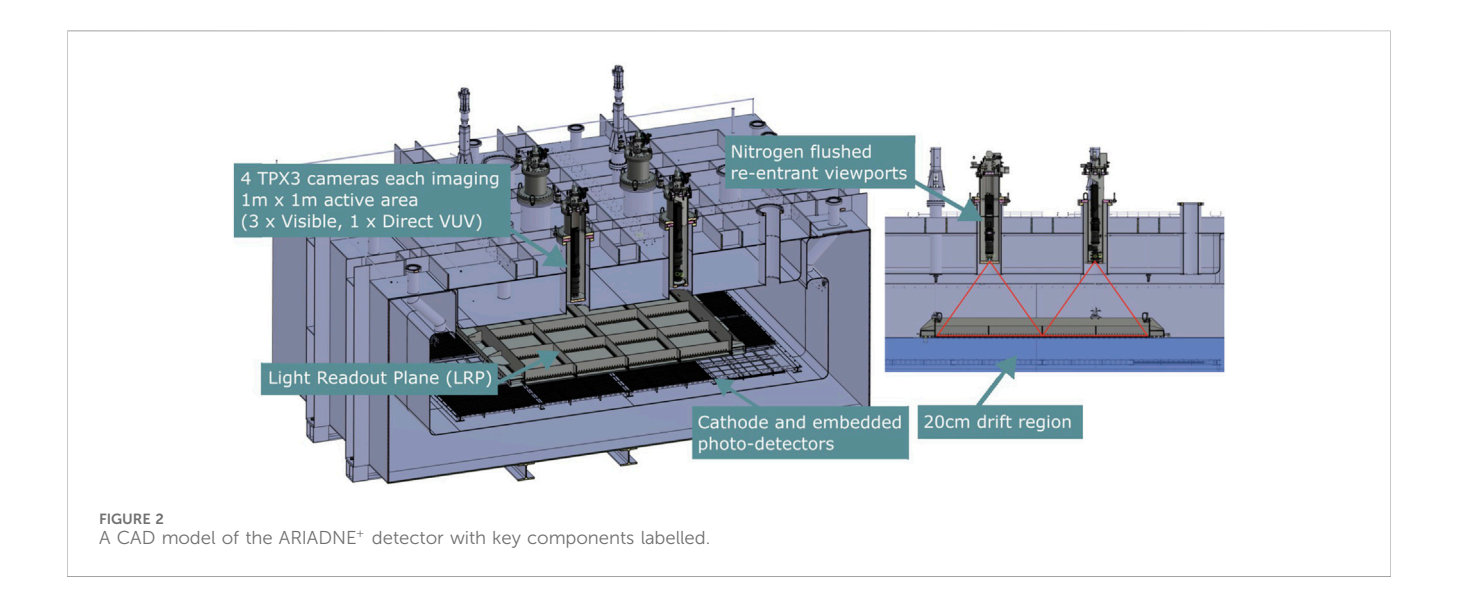
In contrast to traditional LArTPC charge readout approaches, ARIADNE takes advantage of the scintillation light generated by an amplification stage within the detector. When an ionising particle passes through the detector volume, electrons are liberated from argon atoms and primary scintillation light (S1) is emitted. This primary scintillation light can be detected and used to give a T₀ time for the event. The liberated electrons are drifted towards the liquid surface where, for ARIADNE optical readout, they are extracted from the liquid before undergoing amplification within a THGEM. By achieving electric field strengths of 10s of kV/ cm within the THGEM holes, those electrons which are drawn into the THGEM holes undergo Townsend avalanche. This amplification results in ionisations/excitations of gas argon molecules producing secondary scintillation light (S2). The light that is generated from the excitation of argon gas molecules by the amplified drift charge is wavelength shifted before being imaged by the ultrafast Timepix3 camera. The detection principle is shown in Figure 1.

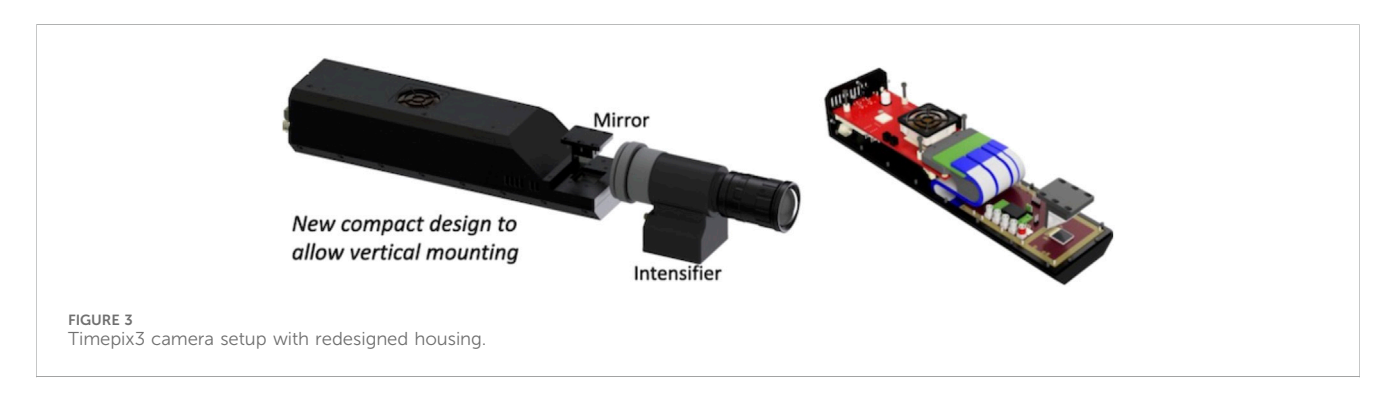
Given the optical nature of the readout, a wide range of commercial/off-the-shelf lenses and optical components can be utilised to control the Field-Of-View (FoV), spatial resolution, etc. Each hit the sensor records provides the X,Y position of the hit along with a 1.6ns resolution timestamp (Time of Arrival - ToA) and a 10-bit intensity value (Time over Threshold - ToT). This intensity value is a result of charge accumulation in the pixel electronics which discharges at a constant rate until the amount drops below a set threshold; at this point a ToT value is then determined. Given that the drift velocity of the detector is known, the X,Y and ToA allow for a full 3D reconstruction which can be combined with the S1 T₀ signal for reconstructing the absolute z position of the event within the drift volume.

The readout is 'Event-Based', or data-driven, meaning that only the pixels registering a hit have their data saved so that all data is zero suppressed as standard. This provides for continuous, trigger-free readout and real-time viewing of data-stream. The Timepix3 chip itself is comprised of 256×256 pixels, $55~\mu m$ square with a maximum readout rate of 40 Mhits/s/cm $^{-2}$. In order to overcome the noise threshold of the Timepix3 ASIC (approximately 500 electrons), the sensor is coupled to an image intensifier. When combined with an intensifier, gains of 1×10^6 photons per incident photon are possible therefore making the setup sensitive down to the single photon level. To explore the possibility of ARIADNE optical readout without the need for wavelength shifting, a custom-made VUV sensitive image intensifier was integrated to one of the Timepix3 cameras.

Since the cameras are mounted on the outside of the TPC, the readout is completely decoupled from the internal TPC electronics, protecting it from any noise induced by the high voltages of the field cage or cathode. In addition, the technology can be easily accessed for maintenance and future upgrades. For example, Timepix4 has an improved timing resolution of approximately 200ps and larger sensor size of 448×512 pixels (Llopart et al., 2022).

The ability to image a large active area per single camera is a key advantage of the ARIADNE readout. As detailed later in this paper, one visible light intensifier Timepix3 camera was used to image 1 m \times 1 m area of the detector: Each pixel on the camera corresponds to 4 mm \times 4 mm on the THGEM plane. Thus, Timepix3 cameras provide a cost-effective readout solution, especially as the detector readout area scales up.





2.2 The ARIADNE⁺ detector components

The next-generation of large scale liquid argon neutrino detectors, such as DUNE, present a number of technological challenges and have large potential to benefit from novel readout techniques (Abed Abud et al., 2024). Given the aforementioned benefits that ARIADNE readout can provide for LArTPCs, ARIADNE⁺ is designed as a test of possible solutions to the challenges of scaling up the readout for use with ktonne-scale TPCs. The detector is installed in the 5 m \times 5 m "cold box" cryostat with a drift length of approximately 20 cm. Four penetrations in the roof of the "cold box" accommodate the reentrant viewports, each containing a Timepix3 camera. Each reentrant port is continuously flushed with nitrogen, thus preventing the build-up of condensation on the viewport glass. A CAD model of the detector setup can be seen in Figure 2.

2.2.1 Visible image intensifier timepix setup

ARIADNE⁺ optical readout utilises a 2.3 m \times 2.3 m LRP, with each Timepix3 camera coupled with a visible light intensifier, achieving a field-of-view of 1 m \times 1 m active area. For ARIADNE⁺ a custom housing was designed which integrates a right-angled mirror, allowing the setup to be installed vertically within the re-entrant viewports and can be seen in Figure 3. These cameras image the wavelength-shifted light from

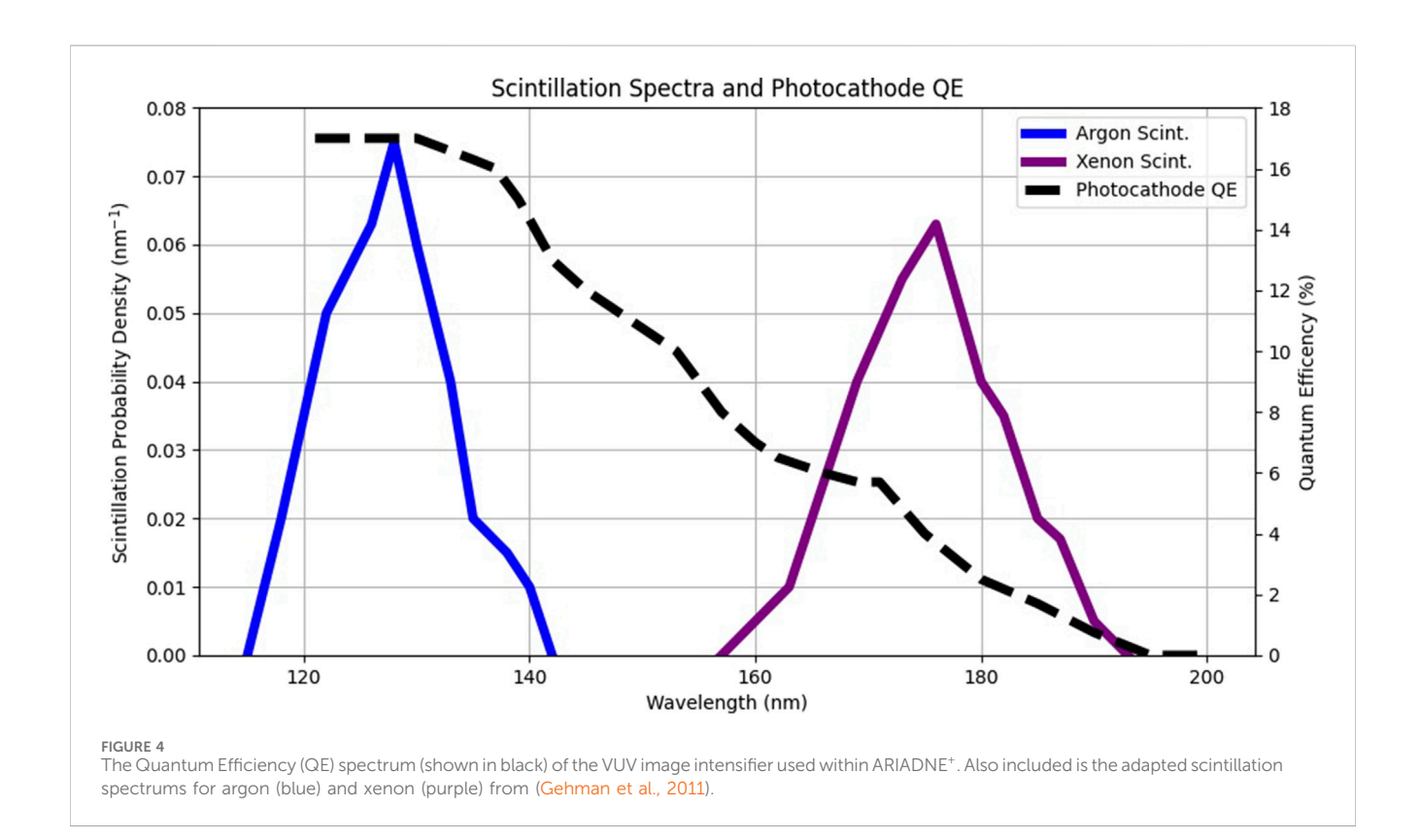
the THGEM using a Voigtländer Nokton 10.5 mm focal length, f/0.95 lens. This light is focused onto the photocathode of a Photonis Cricket intensifier (Photonis, 2025); the light from the intensifier screen is relayed to the Timepix sensor using an Irix Macro lens.

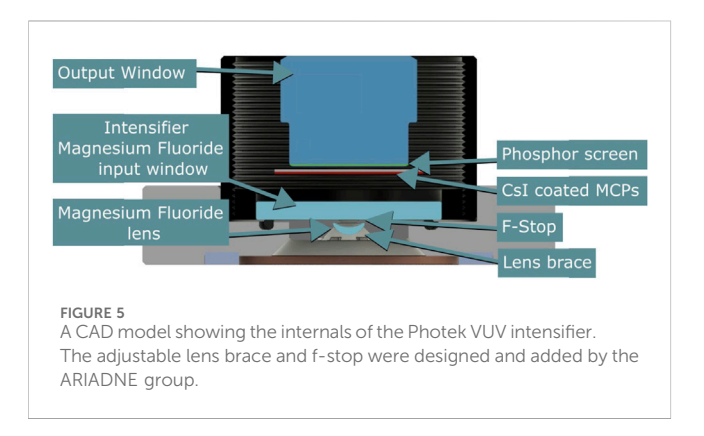
2.2.2 VUV sensitive image intensifier timepix setup

In order to mitigate the need for the use of wavelength shifters and to increase the light collection efficiency, a custom-made VUV sensitive image intensifier was integrated to one of the Timepix3 cameras. The intensifier is able to directly detect the 128 nm secondary scintillation light produced from the THGEMs and this is relayed to the Timepix3 camera.

Image intensifiers are designed to be sensitive to specific wavelengths of interest through tailoring the photocathode, i.e., the Photonis Cricket mentioned earlier is designed for the visible part of the Electromagnetic (EM) spectrum. A prototype image intensifier, with a photocathode sensitive to VUV light, was purchased from Photek (Photek, 2025) for R&D, assessing its feasibility for future runs.

The quantum efficiency of the VUV image intensifier overlaid with the scintillation spectrum of argon can be seen in Figure 4. Included in this figure is also the scintillation spectrum of xenon, highlighting the potential to use this approach within xenon detectors. In particular, the Photonis image intensifier (Byrnes





et al., 2023), has a quoted Quantum Efficiency (QE) of approximately 22% which is an improvement on the approximately 5% achieved by the current Photek intensifier as seen in Figure 4.

Most common lens materials will not transmit VUV wavelengths and so alternative materials for both focusing and the window of the intensifier are needed. For the wavelength of light emitted by argon scintillation, the two best-performing materials available are Lithium fluoride (LiF) and Magnesium fluoride (MgF₂). LiF is particularly sensitive to thermal shock, is hygroscopic and requires extreme care when handling. In comparison, MgF₂ is the hardest of the fluoride materials when used in optics and especially durable in harsh conditions such as those of a LArTPC (KnightOptical, 2025), making it the material of choice for this test. Even as the best performing lens materials for VUV light, the transmittance of MgF₂ and LiF is poor

(approximately 60% (Horiba, 2025)). Thus, the use of multiple stages within the lens is not practical while maintaining optical throughput.

The layout of the intensifier itself is presented in Figure 5. The Caesium Iodide (CsI) coated Microchannel Plates (MCPs) are 18.8 mm in diameter and 4.171 mm from the back of the input window. Mounted to the MCPs is the phosphor screen which again is 18.8 mm in diameter. It is this screen that the Timepix3 is focused on for readout.

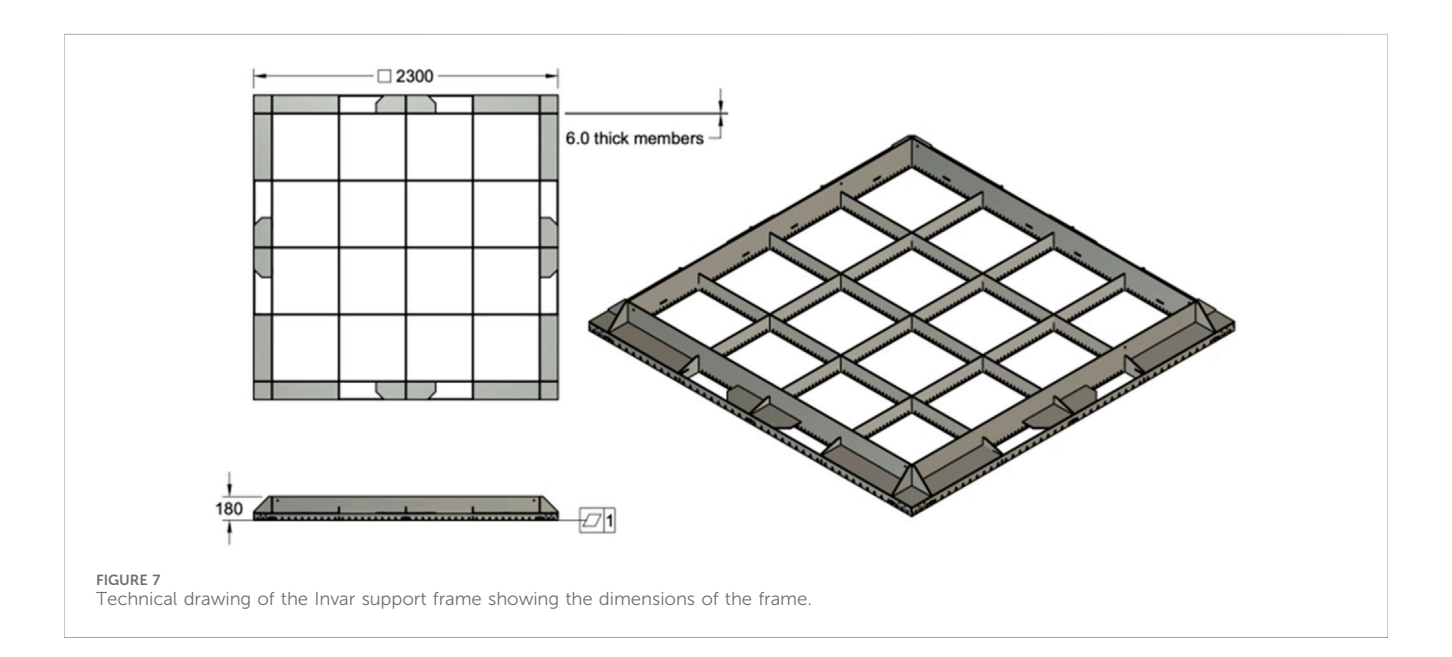
The lens design was based on the following constraints; dimensions of the intensifier, the size of the photocathode, the height above the LRP the lens will sit and the desired field-of-view. The final lens used in the setup is 5 mm in diameter, 11 mm focal length and operated at a speed of f/3. The Timepix3 coupled to a VUV sensitive light intensifier had a calculated field-of-view $0.8~\mathrm{m} \times 0.8~\mathrm{m}$.

2.2.3 Light readout plane (LRP)

The LRP is the first key component in the ARIADNE⁺ readout chain, responsible for the conversion of the ionised electron signal, extracted from the liquid phase, into secondary scintillation light for detection. There are a number of elements to a successful large-scale dual-phase TPC readout: strict tolerance on flatness to ensure a consistent extraction region, good control over the liquid level, modularity for ease of scalability and good understanding of behaviour of the structure in cryogenic conditions to maintain the flatness and the liquid gap.

The LRP consists of the extraction grids, glass-THGEMs and Wavelength Shifting (WLS) polyethylene naphthalate (PEN) layer which are all fixed at well-defined positions within the structure. Figure 6 shows the LRP support frame and a cross-section of the structure.







2.2.4 Invar support frame

The support frame is designed to keep the three layers of the LRP at the correct distance from each other as the structure cools to cryogenic temperatures (LAr is $-185\,^{\circ}$ C). In addition, the structure minimises the stress on the glass as the structure cools.

In order to minimise the stress on the glass components, the coefficients of thermal expansion (α) are as closely matched as possible between that of the glass and the support structure. For the Borofloat 33 THGEMs, α is given as 3.25×10^{-6} m/m °C (Schott, 2024). In comparison, 316 Stainless Steel has a thermal expansion coefficient of 1.6×10^{-5} m/m °C which, given the large temperature change down to -185 °C, has the potential to apply large differential movement to the Borofloat33 components. Invar, on the other hand, an alloy comprised of 64% Iron and 36% Nickel (Efinea Metals, 2024), has a uniquely low coefficient of thermal expansion of 1.2×10^{-6} m/m °C. Therefore, as Invar cools to cryogenic temperatures, the Borofloat 33 THGEMs are subject to less differential movement minimising any resulting stress. A stainless steel frame would contract more than the Borofloat 33 THGEMs, and risk causing excess stress around the edges of the THGEMs.

The frame itself is constructed out of 22 individual Invar parts, waterjet-cut from larger blanks. The blanks were all machined to a thickness of 6.0±0.2 before being sent for waterjet-cutting. Once cut, the individual pieces were then sent to Durham Sheet Metal Works (Metal, 2025) for fabrication. The welding was performed on a large surface

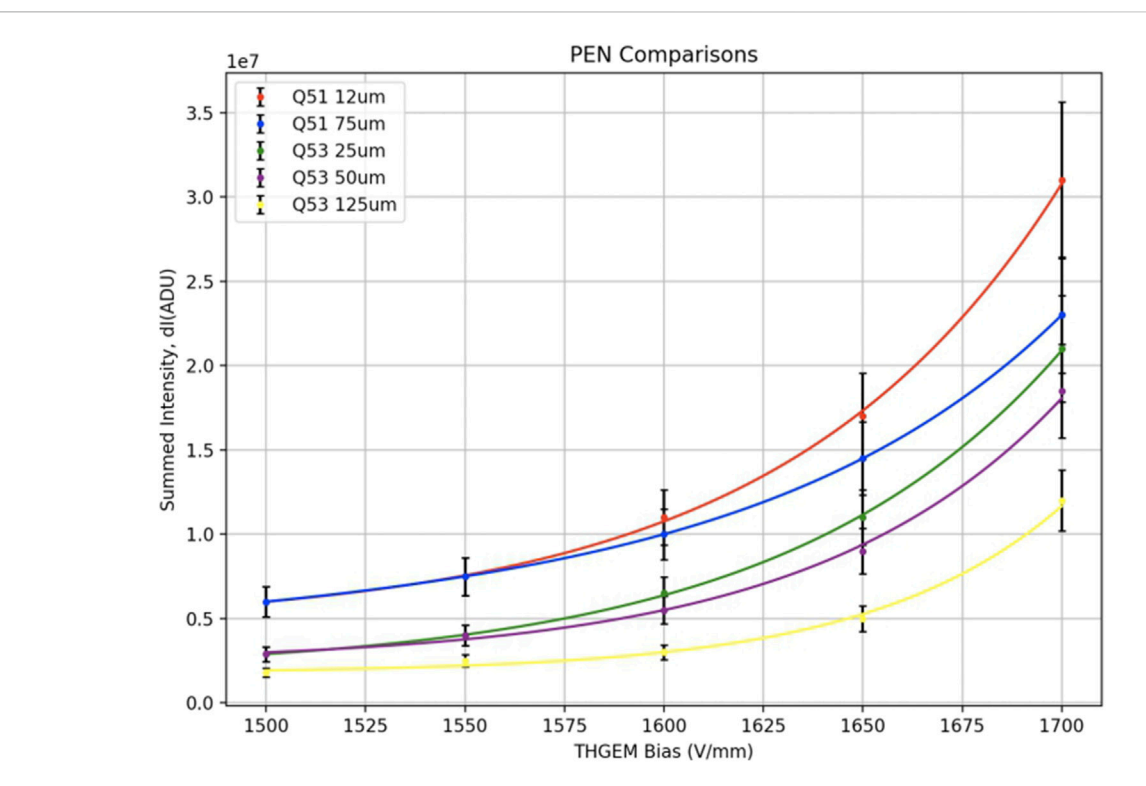


FIGURE 9
This figure shows a selection of the summed intensity of light, using an alpha source, for different grades and thicknesses of PEN film in tests conducted at Liverpool using the 40L demonstrator vessel. This figure was taken from (Philippou, 2022).



(Left) The roof of the "cold box" with the four camera penetrations in the centre and surrounding those the four lifting hooks that the LRP is suspended from. (Right) Lifting the roof with the LRP attached on the bottom side into the trench where the cryostat is located.

plate with focus on ensuring the flatness of the final fabricated LRP structure. A technical drawing of the LRP is shown in Figure 7.

To secure the layers of the LRP into the support structure, a set of PEEK pieces are fastened into holes cut into the frame. The Invar frame consists of 16 segments, within each of these segments the PEEK pieces alternate between those which support the extraction grid and those that secure in place the THGEMs and WLS layers.

2.2.5 Extraction grid

For ARIADNE⁺, the extraction grid was formed using chemically-etched, 0.15 mm thick, stainless steel sheets which are modular in design. Each of the mesh components were tensioned individually with multiple points of attachment to the support frame. The finished extraction grid can be seen in Figure 8. In addition, the distance from the grid to the THGEM was increased from ProtoDUNE-DP's 10 mm (Chardonnet, 2020) to 15 mm to

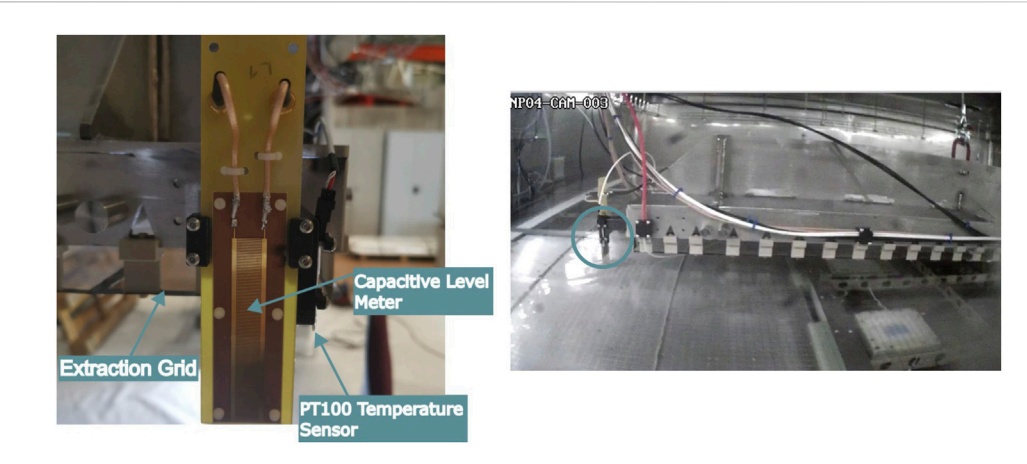
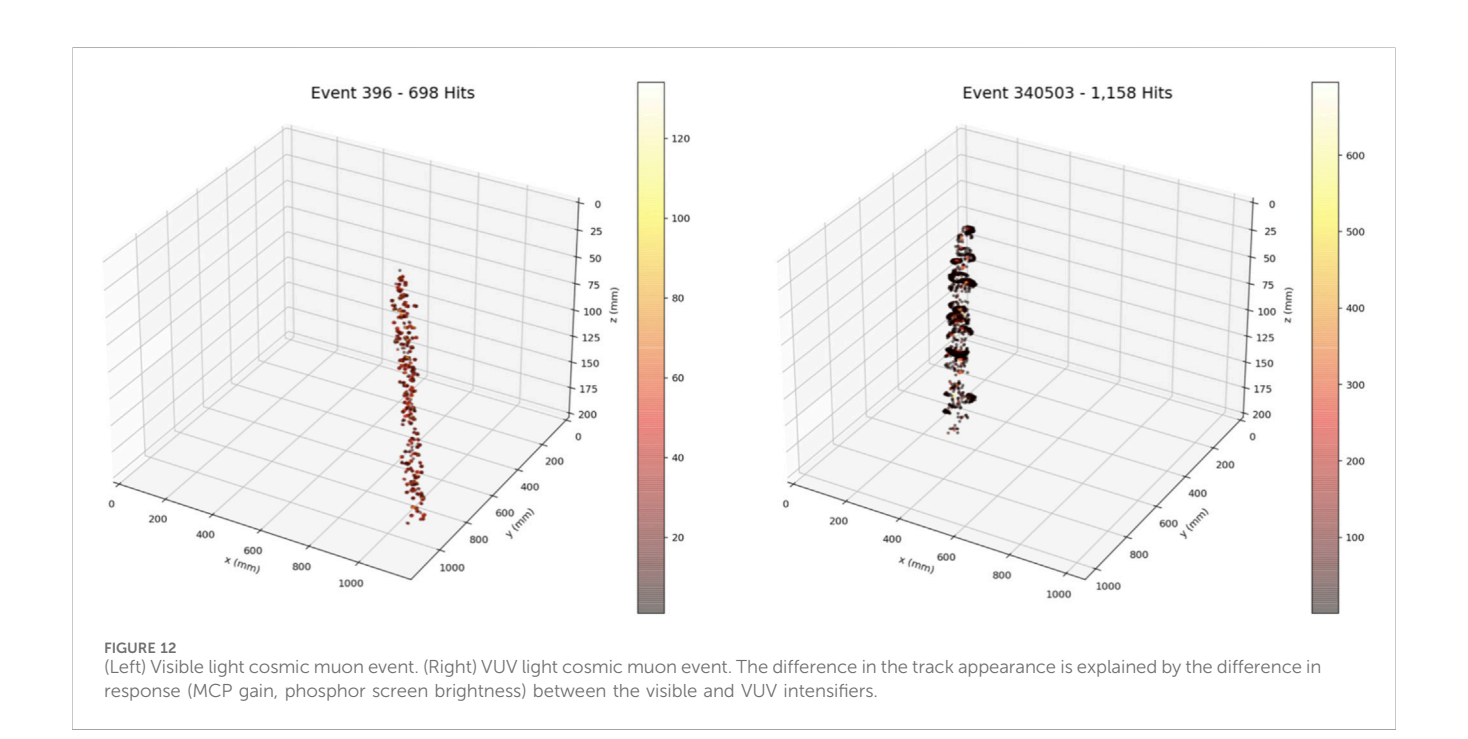


FIGURE 11 (Left) The liquid argon level sensing at each corner of the LRP. (Right) View of the inside of the "cold box", during filling, with one corner PT100 and level sensor circled. The red cable visible is the high voltage supply for the extraction grid.



minimise sensitivity to the effects of any potential disturbance at the liquid surface.

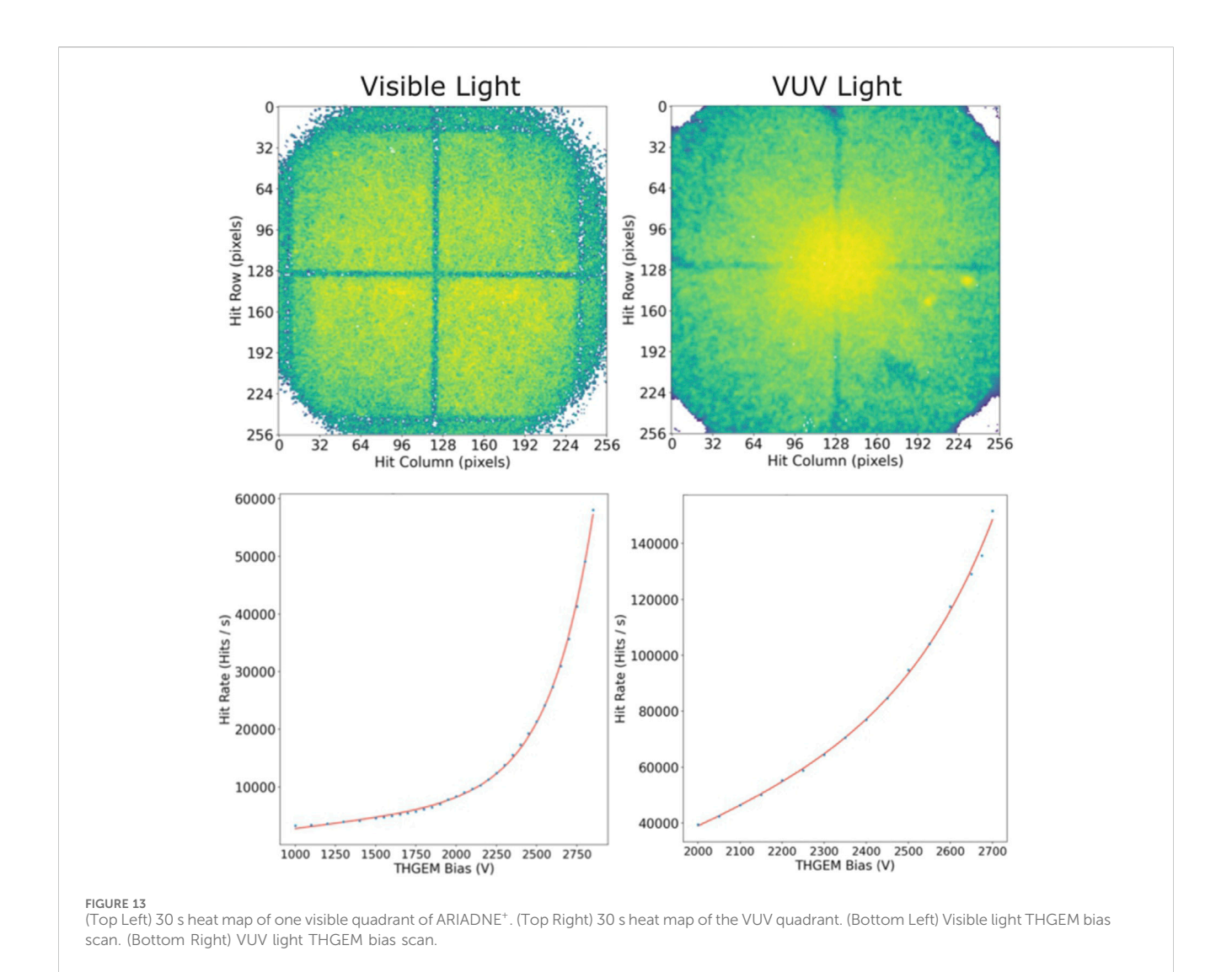
For the entire ARIADNE⁺ run, the extraction grid was maintained at -6 kV with no observed instabilities/sparking issues.

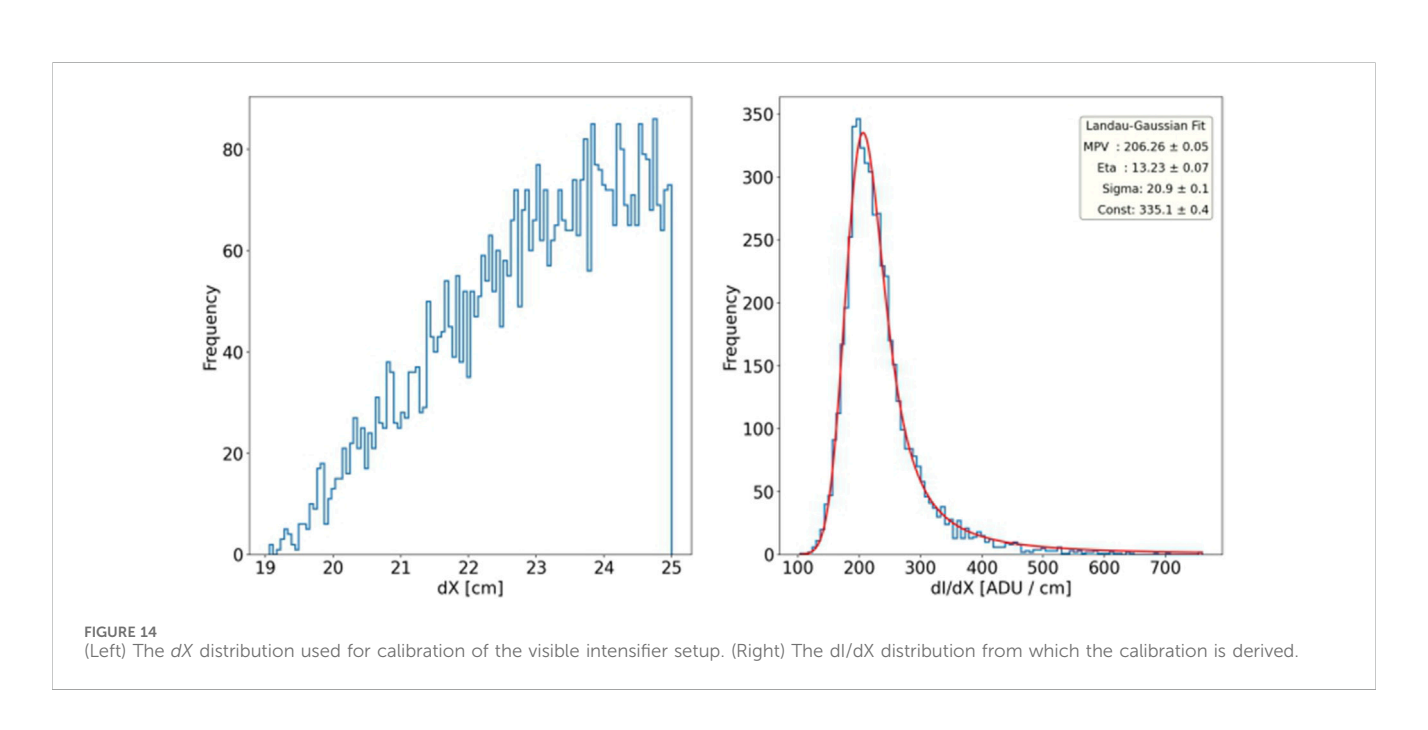
2.2.6 Glass-THGEMs

The ARIADNE⁺ LRP consists of 16 Borofloat 33 THGEMs which are produced using a masked, abrasive machining process (developed by the ARIADNE group). Further details on this novel manufacturing process, and results of prototype testing can be found in (Lowe et al., 2021). The abrasive process produces biconical shaped through-holes which provide a larger surface area on which electrons can accumulate compared to traditional straight through-holes produced in FR4-based THGEMs. This in

turn increases the electric field within these holes without increasing the applied bias, therefore resulting in larger gain-factors and light production. All of the glass-THGEMs produced so far within ARIADNE use a conducting Indium Tin Oxide (ITO) coating as the electrodes. ITO was chosen as it is readily commercially available and inexpensive. In addition, the resistive nature of ITO may reduce the size of discharges, when they occur, by limiting the current flow. For ARIADNE THGEMs, approximately 150 $\Omega/{\rm Sq}$ of ITO is coated on either side of the glass before machining.

The THGEMs were electrically interconnected using copper tabs that link groups of four THGEMs together. Each THGEM had one top connection and one bottom connection to the adjacent THGEM in each group of four. This arrangement can be seen in Figure 8.





2.2.7 Wavelength shifting layer

ARIADNE $^+$ used twelve 50 cm \times 50 cm, 1.1 mm thick sheets of glass with a layer of PEN film glued to one side using a thin layer of optical adhesive. This WLS layer was mounted 1 mm above the topside of the THGEM, with the PEN face towards the THGEM.

Given the close match between the emission spectra for PEN and tetraphenyl-butadiene (TPB) wavelength shifters (discussed in detail within (Kuźniak et al., 2019)), the group has investigated various grades of PEN for use within ARIADNE+. Although the TPB conversion efficiency is better than PEN, there are a number of complexities associated with TPB coatings. TPB comes in a powder and in order to coat an object the powder must be heated in a vacuum evaporation chamber along with the object to be coated; this puts limits on the size of the object being coated. In addition, exposure to ambient light reduces the effectiveness of the TPB over time, which brings additional construction and operational challenges. PEN, on the other hand, is a commercially-available product which can be purchased in rolls or films of various thicknesses and grades - this can be glued to a surface using optically-transparent adhesive. For ARIADNE+, given the manufacturing benefits of using PEN for WLS and complexities with TPB applications, the decision was made to use PEN for the WLS layer.

Testing of different grades and thicknesses of PEN, in order to decide which one to use within ARIADNE⁺, was carried out at Liverpool using the 40L demonstrator vessel (Mavrokoridis et al., 2014). The summed light intensity (measured in Analogue-to-Digital Units) was plotted for five increasing THGEM biases and can be seen in Figure 9. THGEM behaviour is modelled using a convoluted linear-exponential function as seen in Equation 1.

$$S = p_0 x (1 + (p_1 e^{P_2 x})) + p_3$$
 (1)

The largest summed intensity came from the Q51 12 μm film. However, the 12 μm thickness is susceptible to tearing when applied to glass. The next thickness of Q51 available, 75 μm , was found to have a slight reduction in summed intensity but the increase in thickness made it possible to reproduce coated glass panels successfully. This made Q51, 75 μm PEN film the thickness and grade of choice for WLS in ARIADNE⁺.

2.3 Cathode and ARAPUCAS

The "cold box" cathode is a wire-mesh frame supported by a combination of stainless steel and PTFE, which is connected to a power supply capable of up to −30 kV. Embedded within the cathode are a combination of X-ARAPUCAS and ARAPUCA cells (Machado and Segreto, 2016), which are novelly powered over fibre (Arroyave et al., 2024). ARAPUCAS are the photocells chosen for the first two DUNE modules after their successful runs in both ProtoDUNEs.

2.4 Detector commissioning and operation

Once constructed, the LRP was suspended from the roof of the "cold box" via four stainless steel cables, the height of which can be individually adjusted using four cranks on the lid of the cryostat. In Figure 10, the cables for suspending the LRP underneath the lid are shown. The second image shows the LRP secured under the roof

before it was lifted on top of the "cold box". It was then secured on top of the "cold box" vessel before argon-flushing to remove the trapped impurities. Once this was complete, filling with LAr commenced.

The purified LAr was fed from ProtoDUNE-DP into the "cold box". This liquid comes filtered by the CERN cryogenic facility and purity is monitored using a Si-PM, mounted on the side of the "cold box". The purity was continuously monitored and the electron lifetime maintained at approximately 0.5 ms. When the purity dropped below this value the vessel was emptied and refilled this was done twice during the initial 3 weeks of running.

2.4.1 LRP levelling

For efficient dual-phase operation of the detector, it was necessary to maintain the liquid level at approximately halfway between the extraction grid and THGEM in the 15 mm gap. In order to achieve this, the LRP has a PT100 temperature sensor and a capacitance level meter at each corner as shown in Figure 11. The PT100s are positioned in line with the extraction grid and are crucial for ensuring the LRP was level before lowering the structure.

Once the first PT100 was reading LAr temperature, it was then known that the liquid has reached the level of the extraction grid at that position. The filling was then stopped and it was now important to ensure that the LRP is level to the liquid surface. At this stage, the height of the LRP was controlled by hand cranks. By using these hand cranks, the height was adjusted at each corner of the LRP so that all PT100s are measuring liquid temperature. Monitoring was then switched to a combination of the webcam installed in the "cold box", also seen in Figure 11, and the capacitance level meters (part of the slow control system provided by CERN). The main use of the capacitance meters is for ensuring that all four sides are being lowered at the same rate (relative distance measurement was performed).

2.4.2 TPC biasing

With the cathode voltage set at $-15~\rm kV$ and the extraction grid biased to $-6\rm kV$, the THGEMs were then biased (typically $-2.7~\rm kV$). After initially biasing the THGEMs, it was found that grounding the top of the THGEMs and adjusting the bias on the bottom of each quadrant was best for achieving the highest stable THGEM potential.

3 Results

Data collection for the first ARIADNE⁺ run consisted of 3 weeks of cosmic data. The analysis presented here utilises data collected from one visible light camera and one VUV light sensitive camera.

3.1 Gallery of events

Presented in Figure 12 are a selection of events from two quadrants of the ARIADNE⁺ detector, imaged with a visible light and VUV light camera. For the visible light setup, it was determined that each pixel was imaging approximately 4 mm of the THGEM plane. For the VUV sensitive light setup, using the calculated FoV, each pixel is imaging approximately 3.125 mm of the THGEM plane.

Due to the short electron drift length of the detector the tracks are approximately 20 cm.

3.2 Cosmic muon analysis

For the visible and VUV quadrant of the detector, a number of analyses were conducted, the results of which can be seen in Figures 13, 14. A heat map was first produced from 30 s of raw hits. In both heat maps the Invar frame is visible, illustrating the amount of light produced in a short frame of time as well as verifying the field-ofview. The FoV for the visible light intensifier setup was determined to be approximately 1.1 m \times 1.1 m, determined using the known dimensions of the Invar frame visible in the image. For the VUV light sensitive imaging setup, edges of the Invar frame are not visible, but the FoV was calculated as approximately 0.8 m \times 0.8 m using the known magnesium fluoride lens characteristics. A THGEM bias scan for both quadrants is also presented in this figure.

Finally, by using a selection of clustered through-going muon events (those that traverse the majority of the drift region), it is possible to obtain a calibration for the detector. Clustered events are groups of hits that fall within limits set by the user based on pixel separation in X,Y and ToA. Each event's measured light intensity (dI) is divided by it's length (dX) in order to produce a dI/dX distribution as seen in Figure 14. This analysis was not conducted using the VUV data due to the heavy vignetting present; future work will look at correcting this effect and exploring the switch from refractive to reflective optics.

The Most-Probable-Value (MPV) of the Landau-Gaussian fit applied to the data (as seen in Figure 14) can be equated to the known deposition rate for cosmic muons in liquid argon (2.12 MeV/cm) to determine a calibration. For the visible light intensifier data, the Analogue-to-Digital Unit (ADU) per MeV is determined to be (100.15 \pm 0.05) (stat.). In order to calculate the energy resolution of the dataset, the widths of the Landau (η) and Gaussian (σ) fits are added in quadrature and expressed as a fraction of the MPV; the Gaussian component is used to represent variations in the detector response. The energy resolution is given by Equation 2.

Energy Resolution (%) =
$$\frac{\sqrt{\eta^2 + \sigma^2}}{MPV} * 100$$
 (2)

Using the fits seen in Figure 14, the energy resolution was calculated to be approximately 11.5%.

4 Discussion

This paper provides a comprehensive overview of the ARIADNE⁺ experiment conducted at the CERN Neutrino Platform, highlighting its successful operation and key results. Optical readout offers high resolution data collection that is completely decoupled from the internal TPC electronics. Timepix3 cameras have native 3D readout with data-driven readout as standard which provides zero suppression. Through the use of optics, a spatial resolution at the millimetre level has been demonstrated with 1.6ns timing resolution.

The ARIADNE⁺ LRP comprises the largest glass-THGEM array constructed to date with an active area of 2 m \times 2 m. These glass-

THGEMs are manufactured via an abrasive machining process which produces biconical shaped holes, benefiting the overall light output. Discussed was the reasoning behind the choice of Invar for the LRP support frame and the decision to use PEN film for wavelength shifting instead of the conventional TPB used in detectors of this type. A chemically etched, modular extraction grid was installed with each sheet being tensioned individually. The grid was maintained at a constant -6 kV during operation with no observed discharge issues.

By collecting cosmic muon data, the FoV for the cameras (1.1 m \times 1.1 m for the visible intensifier setup and 0.8 m×0.8 m for the VUV sensitive setup) was verified and an energy calibration was preformed using the visible light intensifier data. ARIADNE+ saw, for the first time in a detector of this type, imaging and tracking using pure VUV light. The image obtained with the MgF $_2$ lens shows strong evidence of vignetting and further study in the future into the design of the VUV optics will be required. Furthermore, a detailed simulation of the optical system can aid with the correction to the vignetting. Nevertheless, these results demonstrate the potential of such technology when utilised in such a way.

Planning is currently taking place for the next test of this technology on an even larger scale relevant for DUNE. This would see the ProtoDUNE NP-02 cryostat instrumented with an 6 m \times 3 m active area optical readout with a combination of Timepix3/Timepix4 cameras and high sensitivity photodetectors. Each LRP is planned to be approximately the same dimensions as the DUNE CRPs meaning integration into a DUNE module will be similar to that of the CRPs.

The ARIADNE project has demonstrated the scalability of this high resolution, ultra-fast optical readout. The ability to image large areas of the detector with very few cameras makes this a cost-effective readout method without sacrificing physics capabilities. The number of cameras required to instrument a DUNE fardetector will depend on the desired spatial resolution for each camera. For example, 320 Timepix4 cameras will be able to image the $60~\text{m} \times 12~\text{m}$ far-detector surface area with 3 mm/ pixel resolution. ARIADNE technology is now considered an option for use within the remaining two far detectors as part of DUNE Phase-II (Abed Abud et al., 2024).

Data availability statement

The raw data supporting the conclusions of this article will be made available by the authors, without undue reservation.

Author contributions

PM: Writing – review and editing. AD: Writing – review and editing. HG: Writing – review and editing, Supervision. DG-D: Writing – review and editing. AL: Writing – original draft, Writing – review and editing. KrM: Writing – review and editing. KoM: Writing – original draft, Writing – review and editing. MN: Writing – review and editing. BP: Writing – review and editing. FP: Writing – review and editing. SR: Writing – review and editing. AR: Writing – original draft. FR: Writing – review and editing. AR: Writing – original draft, Writing – review and editing. AH: Writing – review and editing. CT: Writing – review and editing. JV: Writing – review and editing.

Funding

The author(s) declare that financial support was received for the research and/or publication of this article. This research was funded by STFC UKRI Grant No. ST/T007265/1 and ARIADNE ERC Grant No. 677927.

Acknowledgments

The authors would like to thank the members of the Mechanical Workshop of the University of Liverpool's Physics Department, for their contributions and invaluable expertise. The authors would also like to thank the members of the CERN Neutrino Platform cryogenic team.

Conflict of interest

The authors declare that the research was conducted in the absence of any commercial or financial relationships that could be construed as a potential conflict of interest.

References

Abed Abud, A., Abi, B., Acciarri, R., Acero, M., Adames, M., Adamov, G., et al. (2024). DUNE phase II: scientific opportunities, detector concepts, technological solutions. *J. Instrum.* 19, P12005. doi:10.1088/1748-0221/19/12/p12005

Arroyave, M., Behera, B., Cavanna, F., Feld, A., Guo, F., Heindel, A., et al. (2024). Characterization and novel application of power over fiber for electronics in a harsh environment. *J. Instrum.* 19, P10019. doi:10.1088/1748-0221/19/10/p10019

Byrnes, N., Parmaksiz, I., Adams, C., Asaadi, J., Baeza-Rubio, J., Bailey, K., et al. (2023). Next-crab-0: a high pressure gaseous xenon time projection chamber with a direct vuv camera based readout. *J. Instrum.* 18, P08006. doi:10.1088/1748-0221/18/08/p08006

Chardonnet, E. (2020). The dune dual-phase liquid argon tpc. J. Instrum. 15, C05064. doi:10.1088/1748-0221/15/05/c05064

DUNE Collaboration (2018). The DUNE far detector interim design report volume 1: physics, technology and strategies. arxiv Preprint.

DUNE Collaboration (2023). The DUNE far detector vertical drift technology, technical design report. arxiv Preprint.

Efinea Metals (2024). Invar® and free-cut Invar"36"® alloy fm properties.

Fisher-Levine, M., and Nomerotski, A. (2016). Timepixcam: a fast optical imager with time-stamping. *J. Instrum.* 11, C03016. doi:10.1088/1748-0221/11/03/c03016

Gehman, V., Seibert, S., Rielage, K., Hime, A., Sun, Y., Mei, D. M., et al. (2011). Fluorescence efficiency and visible re-emission spectrum of tetraphenyl butadiene films at extreme ultraviolet wavelengths. *Nucl. Instrum. Methods Phys. Res. Sect. A Accel. Spectrom. Detect. Assoc. Equip.* 654, 116–121. doi:10.1016/j.nima.2011.06.088

Hollywood, D., Majumdar, K., Mavrokoridis, K., McCormick, K., Philippou, B., Powell, S., et al. (2020). Ariadne—a novel optical lartpc: technical design report and initial characterisation using a secondary beam from the cern ps and cosmic muons. *J. Instrum.* 15, P03003. doi:10.1088/1748-0221/15/03/p03003

Horiba (2025). What detector can be used together with a vuv system? Minami-ku, Japan: Horiba. Available online at: https://www.horiba.com/int/scientific/technologies/vacuum-ultra-violet-spectroscopy/vuv-system-detector/.

Knight Optical (2025).
 $Custom\ magnesium\ fluoride.$ North Kingstown, Rhode Island: Knight Optical. The reviewer MB declared a past collaboration with the author DGAD to the handling editor.

Generative AI statement

The author(s) declare that no Generative AI was used in the creation of this manuscript.

Any alternative text (alt text) provided alongside figures in this article has been generated by Frontiers with the support of artificial intelligence and reasonable efforts have been made to ensure accuracy, including review by the authors wherever possible. If you identify any issues, please contact us.

Publisher's note

All claims expressed in this article are solely those of the authors and do not necessarily represent those of their affiliated organizations, or those of the publisher, the editors and the reviewers. Any product that may be evaluated in this article, or claim that may be made by its manufacturer, is not guaranteed or endorsed by the publisher.

Kuźniak, M., Broerman, B., Pollmann, T., and Araujo, G. (2019). Polyethylene naphthalate film as a wavelength shifter in liquid argon detectors. *Eur. Phys. J. C* 79, 291–296. doi:10.1140/epjc/s10052-019-6810-8

Llopart, X., Alozy, J., Ballabriga, R., Campbell, M., Casanova, R., Gromov, V., et al. (2022). Timepix4, a large area pixel detector readout chip which can be tiled on 4 sides providing sub-200 ps timestamp binning. *J. Instrum.* 17, C01044. doi:10.1088/1748-0221/17/01/c01044

Lowe, A., Majumdar, K., Mavrokoridis, K., Philippou, B., Roberts, A., Touramanis, C., et al. (2020). Optical readout of the ariadne lartpc using a timepix3-based camera. *Instruments* 4, 35. doi:10.3390/instruments4040035

Lowe, A., Majumdar, K., Mavrokoridis, K., Philippou, B., Roberts, A., and Touramanis, C. (2021). A novel manufacturing process for glass thgems and first characterisation in an optical gaseous argon tpc. *Appl. Sci.* 11, 9450. doi:10.3390/app11209450

Machado, A., and Segreto, E. (2016). Arapuca a new device for liquid argon scintillation light detection. J. Instrum. 11, C02004. doi:10.1088/1748-0221/11/02/c02004

Majumdar, K., and Mavrokoridis, K. (2021). Review of liquid argon detector technologies in the neutrino sector. *Appl. Sci.* 11, 2455. doi:10.3390/app11062455

Mavrokoridis, K., Ball, F., Carroll, J., Lazos, M., McCormick, K., Smith, N., et al. (2014). Optical readout of a two phase liquid argon tpc using ccd camera and thgems. *J. Instrum.* 9, P02006. doi:10.1088/1748-0221/9/02/p02006

Metal, D. S. (2025). Durham sheet metal. South Shields: DSM.

Philippou, B. (2022). Design, construction and initial characterisation of Ariadne-A novel dual-phase LArTPC with an optical readout system, and development towards light readout planes for optical, large-scale, dual-phase, LArTPCs within the neutrino sector. Liverpool, United Kingdom: University of Liverpool. Ph.D. thesis.

Photek (2025). Photek. East Sussex, UK: Photek. Available online at: https://www.photek.com/.

Photonis (2025). CricketTM2 advanced image intensifier adapter. Brive-la-Gaillarde, France: Photonis. Available online at: https://www.photonisdefense.com/Cricket-Advanced-Image-Intensifier-Adapter.

Schott (2024). Borofloat® 33 – thermal properties. Mainz, Germany: Schott.